Cisplatin Preferentially Binds Mitochondrial DNA and Voltage-Dependent Anion Channel Protein in the Mitochondrial Membrane of Head and Neck Squamous Cell Carcinoma: Possible Role in Apoptosis

Zejia Yang,[1] Lisa M. Schumaker,[1] Merrill J. Egorin,[2] Eleanor G. Zuhowski,[2] Zhongmin Guo,[1] and Kevin J. Cullen[1]

Abstract

Purpose: Cisplatin adducts to nuclear DNA (nDNA) are felt to be the molecular lesions that trigger apoptosis, but the mechanism linking nDNA adduct formation and cell death is unclear. Some literature in the last decade has suggested a possible direct effect of cisplatin on mitochondria independent of nDNA interaction. In this study, we define separately the sequelae of cisplatin interactions with nDNA and with mitochondria in head and neck squamous cell carcinoma (HNSCC) cell lines.

Experimental Design: Cisplatin binding to mitochondrial DNA (mtDNA) and proteins was analyzed by atomic absorption spectroscopy and other methods.

Results: Following 1 hour of exposure to cisplatin, platinum adducts to mtDNA were 300- to 500-fold more abundant than adducts to nDNA; these differences were not due to differences in rates of adduct repair. Whereas HNSCC cell cytoplasts free of nDNA retained the same dose-dependent cisplatin sensitivity as parental cells, HNSCC ρ^0 cells free of mtDNA were 4- to 5-fold more resistant to cisplatin than parental cells. Isolated mitochondria released cytochrome *c* within minutes of exposure to cisplatin, and ultrastructural analysis of intact HNSCC cells by electron microscopy showed marked mitochondrial disruption after 4 hours of cisplatin treatment, whereas the nucleus and other cellular structures remain intact. The very prompt release of cytochrome *c* from isolated mitochondria implies that apoptosis does not require alteration in mitochondrial gene transcription. Further, cisplatin binds preferentially to mitochondrial membrane proteins, particularly the voltage-dependent anion channel.

Conclusions: Cisplatin binding to nDNA is not necessary for induction of apoptosis in HNSCC, which can result from direct action of cisplatin on mitochondria.

Cisplatin [*cis*-diamminedichloroplatinum II (CDDP)] has been in widespread clinical use for more than a generation and is one of the most important chemotherapeutic agents ever introduced. Despite the importance of cisplatin in the treatment of head and neck cancer and a broad range of other malignancies, there are many uncertainties about its molecular pharmacology and ultimate mechanism of action. This has been an area of very active investigation for >2 decades.

Upon entering the low chloride intracellular environment, cisplatin is hydrated to form a positively charged species, which can react with nuclear DNA (nDNA) and other nucleophilic species within the cell (1).

Cisplatin has been most extensively characterized as a DNA-damaging agent, and the cytotoxicity of cisplatin has generally been attributed to the ability to form interstrand and intrastrand nDNA cross-links. Formation and repair of these cisplatin/nDNA adducts have been widely studied for the last 2 decades. For some time after the introduction of cisplatin, its cytotoxicity was felt to result from inhibition of DNA synthesis by cisplatin/DNA adducts, but several lines of evidence showed that this was not the case (2). More recently, it was shown that tumor cell exposure to cisplatin ultimately results in apoptosis (3, 4). However, the mechanism or mechanisms by which nuclear cisplatin/DNA adducts generate the cytoplasmic cascade of events leading to apoptosis have not been defined.

Although most investigations of the cellular and molecular pharmacology of cisplatin have focused on interactions between cisplatin and nDNA, only ~1% of intracellular platinum is bound to nDNA, with the great majority of the intracellular drug available to interact with nucleophilic sites on other molecules, including but not limited to phospholipids, cytosolic, cytoskeletal and membrane proteins, RNA, and mitochondrial DNA (mtDNA; refs. 5, 6).

Authors' Affiliations: [1]University of Maryland Marlene and Stewart Greenebaum Cancer Center, Baltimore, Maryland and [2]University of Pittsburgh Cancer Institute, Pittsburgh, Pennsylvania

Received 4/27/06; revised 7/14/06; accepted 7/21/06.

Grant support: R01CA90328 and K24CA82238.

The costs of publication of this article were defrayed in part by the payment of page charges. This article must therefore be hereby marked *advertisement* in accordance with 18 U.S.C. Section 1734 solely to indicate this fact.

Requests for reprints: Kevin J. Cullen, University of Maryland Greenebaum Cancer Center, 22 South Greene Street, 9NE17, Baltimore, MD 21201. Phone: 410-328-5506; Fax: 410-328-2578; E-mail: kcullen@umm.edu

doi:10.1158/1078-0432.CCR-06-1037

Further evidence that nDNA adduct formation may not be the sole determinant of cisplatin-induced cytotoxicity comes from recent clinical studies showing that combined therapy with other agents, such as taxanes, significantly enhances the clinical efficacy of cisplatin while actually inhibiting formation of cisplatin adducts with nDNA (7).

Resistance to cisplatin can result from several mechanisms, including decreased uptake, inactivation by nucleophilic compounds, such as glutathione, or accelerated DNA repair (8). Inhibiting glutathione synthesis with buthionine sulfoximine (BSO) has been known for some time to enhance cisplatin cytotoxicity in tumor cells as well as increasing normal cell toxicity (9, 10).

We previously showed that BSO treatment of head and neck tumor cell lines was accompanied by complete loss of detectable glutathione and marked increase in cisplatin cytotoxicity. However, this enhanced apoptotic cell killing was not accompanied by significant changes in cisplatin DNA adduct formation (11).

Overexpression of Bcl-2 is associated with cisplatin resistance in several model systems (12). Recently, we showed that although Bcl-2 transfection was associated with significant acquired cisplatin resistance, it did not produce measurable alterations in nuclear cisplatin/DNA adducts (13). Because of the lack of clarity on the role of nuclear cisplatin/DNA adducts in mediating cytotoxicity and because of the Bcl-2 data suggesting the importance of mitochondrial pathways in cisplatin action, we elected to look more carefully at cisplatin interactions with mitochondria and mtDNA.

Limited studies have examined cisplatin activity in cells selectively depleted of mtDNA, with conflicting results. Loss of mtDNA has been associated with increased sensitivity to cisplatin-induced apoptosis (14), but more recent literature has shown that cells depleted of mtDNA show significant resistance to cell death mediated by a range of chemotherapeutic agents (15). Indeed, mtDNA is significantly more sensitive than nDNA to the damage induced by a range of agents (16).

Recent reports have also shown the ability of various compounds to act directly on mitochondria, inducing loss of membrane potential and release of apoptogenic proteins from isolated mitochondria (17–19). Most recently, such effects are selective, affecting mitochondria from sensitive but not insensitive cells (20–22).

Mitochondrial damage by cisplatin has increasingly been studied as a mediator of toxicity in normal tissues in animals receiving cisplatin. Gastrointestinal toxicity (23), ototoxicity (24), and nephrotoxicity (25, 26) have all been attributed to mitochondrial effects of cisplatin.

In this study, we attempt to define separately the sequelae of the interaction of cisplatin with nDNA and with mitochondria in head and neck cancer cell lines.

Materials and Methods

Reagents. DMEM, phenol red–free DMEM, PBS, trypsin/EDTA, and glutamine were obtained from MediaTech (Herndon, VA). Fetal bovine serum was obtained from Quality Biological, Inc. (Gaithersburg, MD). BSO, CHAPS detergent, cytochalasin B, ethidium bromide, Epon 812 substitute, EDTA, Ficoll, glutathione, HEPES, leupeptin, pepstatin, phenazine methosulfate, phenylmethylsulfonyl fluoride, propidium iodide, sucrose, 5-sulfosalicylic acid, sodium pyruvate, Spurr resin, uridine, and 2,3-bis[2-methoxy-4-nitro-5-sulfophenyl]-2H-tetrazolium-5-carboxanilide inner salt (XTT) were obtained from Sigma-Aldrich (St. Louis, MO). Apopain/CPP32 fluorometric substrate was obtained from Upstate Biotechnology (Lake Placid, NY).

Cell lines. PCI-13 and PCI-51 cells were obtained from Dr. Theresa Whiteside (University of Pittsburgh, Pittsburgh, PA). UMSCC-17B cells were obtained from Dr. Thomas Carey (University of Michigan, Ann Arbor, MI). Cells were routinely maintained in DMEM supplemented with 10% fetal bovine serum and 2 mmol/L glutamine.

Cytoplast production (cell enucleation). Enucleated cells were produced by cytochalasin B treatment and Ficoll centrifugation (27–29). PCI-13 cytoplasts obtained by this method were allowed to recover for 2 hours in a 37°C CO_2 incubator and then incubated for a further 24 hours after the addition of another 2 mL medium containing the indicated dose of cisplatin. For caspase-3 assay, cells and cytoplasts were harvested with trypsin/EDTA, rinsed with PBS, pelleted, and resuspended in 100 to 200 μL lysis buffer [100 mmol/L HEPES (pH 7.5), 10% sucrose, 1 mmol/L EDTA, 0.1% CHAPS, 1 mmol/L phenylmethylsulfonyl fluoride, 10 μg/mL pepstatin, 10 μg/mL leupeptin]. Samples were frozen (−70°C) for 30 minutes and thawed on ice to lyse. Supernatant was recovered by a 5-minute spin in a 4°C microcentrifuge at maximum speed (17,500 × *g*).

Caspase-3 assay. Cell or cytoplast lysate (25 μg protein) and apopain/CPP32 fluorometric substrate (50 μmol/L) were added to buffer [10% sucrose, 0.1% CHAPS, 100 mmol/L HEPES (pH 7.5), 1 mmol/L EDTA] to a total volume of 250 μL and incubated at 37°C for 1 hour. Samples were transferred to a microplate, and fluorescence measurements (excitation, 360 nm/emission, 460 nm) were obtained using a Bio-Tek Synergy HT multimode plate reader (Bio-Tek, Winooski, VT). Results are shown in relative fluorescence units.

Cytochrome c release from isolated rat liver mitochondria. Rat liver mitochondria were isolated as in Bossy-Wetzel (30). Assays were done within 4 hours of isolation. Samples were prepared to examine both caspase-3 activation (data not shown) and cytochrome *c* release; therefore, PCI-13 cell cytosol was included as a source of cellular enzymes for the caspase assay. PCI-13 cytosol was prepared as described (31). Protein concentration for mitochondria and cytosol was determined by modified Bradford assay (Bio-Rad, Hercules, CA). Mitochondria (15 μL, 1 μg/μL protein), PCI-13 cytosol (30 μL, 5 μg/μL protein), and dATP (1 mmol/L) were combined with 5 μL mitochondrial resuspension buffer containing either 1 μmol/L cytochrome *c*, 150 μmol/L Ca^{2+}, the indicated amount of cisplatin, or buffer alone. Samples were incubated at 30°C for 1 hour. Following a brief spin (5 minutes at 17,500 × *g*) to pellet mitochondria, half of the supernatant was loaded onto a SDS-PAGE gel for Western blotting with anti–cytochrome *c* (see below).

Reduced glutathione assay. Reduced glutathione (GSH) was measured based on the enzymatic method of Tietze (32). PCI-13 and PCI-51 cells were plated to 50% confluence in DMEM supplemented with 10% fetal bovine serum and 2 mmol/L glutamine; 100 μmol/L BSO or control medium was added the following day. After 24 hours, cells were trypsinized, washed twice, and resuspended in cold PBS (200 μL per single well of a six-well culture plate). For mitochondrial GSH determination, mitochondria from six T175 flasks (treated with BSO or control as above) were isolated by the protocol described below for DNA purification. Pelleted mitochondria were resuspended in 100 μL PBS. Mitochondria or cells were lysed by the addition of 5% 5-sulfosalicylic acid and placed on ice for 10 minutes. The lysates were cleared by a 10-minute, 4°C spin at 17,500 × *g*. Lysates (25 μg protein) were then used for GSH determination against a standard curve of purified GSH.

Generation and culture of PCI-13 and UMSCC-17B ρ^0 cells. ρ^0 cell lines were derived from PCI-13 and UMSCC-17B cells by the established method of long-term exposure to ethidium bromide (33–37). Cells were cultured in DMEM supplemented with 10% fetal bovine serum, 2 mmol/L glutamine, 1 mmol/L sodium pyruvate, 50 μg/mL uridine, and 50 ng/mL (PCI-13) or 100 ng/mL (UMSCC-17B) ethidium bromide (EB medium). After 12 weeks, elimination of mtDNA was confirmed (see PCR and Western blot methods). mtDNA-depleted cells

were routinely maintained in EB medium; however, for XTT assays, ethidium bromide was omitted to prevent interference with absorbance measurement.

Cytotoxicity assay. Parental and ρ^0 cell lines were plated, in triplicate, in 96-well plates at 7,500 per well in 100 μL modified EB medium (without phenol red and ethidium bromide). Following overnight incubation, 100 μL medium containing cisplatin or irinotecan at the indicated concentrations was added. After 3 to 5 days, 50 μL medium containing 1 mg/mL XTT and 15 μg/mL phenazine methosulfate was added per well. After 1 to 2 hours of further incubation, absorbance was measured at 450 nm and expressed as a percentage of the absorbance reading of control cells (% survival). The IC_{50} and IC_{80} were defined as the concentration of cisplatin causing a 50% and 80% decrease, respectively, in absorbance compared with control. IC_{50} and IC_{80} values were determined using GraphPad Prism (GraphPad Software, San Diego, CA) from a sigmoidal dose-response curve (variable slope) fitted to the plot of % survival versus log [cisplatin].

Clonogenic cell growth assay. The cells were plated in 24-well plates at a density of 200 to 400 per well and incubated overnight to allow the cells to adhere. The following day, the medium was removed from each well and replaced with fresh medium containing different concentrations of CDDP. After incubating in a 37°C CO_2 incubator for 1 hour, the CDDP-containing medium was removed and replaced with normal medium. The cells were further incubated for 7 to 12 days to allow surviving cells to form colonies. To stain the colonies, the cells were incubated for another 24 hours following the addition of *p*-iodonitrotetrazolium violet (final dilution, 0.143 mg/mL). The ProtoCOL colony detection system (Microbiology International, Frederick, MD) was used to count the number of colonies having a minimum diameter of 50 μm. Error bars represent results from triplicate wells for each experimental treatment.

Purification of mtDNA and nDNA and measurement of platination. PCI-13 and PCI-51 cells were treated with 50 μmol/L cisplatin for 1 or 2 hours. For each cell line, cells from 10 T175 flasks were harvested by scraping, washed twice with cold PBS, and resuspended in 4 to 5 mL chilled homogenizing buffer [250 mmol/L sucrose, 10 mmol/L EDTA, 30 mmol/L Tris-HCl (pH 7.5)]. Cells were homogenized by motorized pestle in a glass homogenizer. Nuclei were pelleted at 1,000 × *g* for 1 minute at 4°C, and nDNA was purified using the PureGene DNA Isolation Cell and Tissue kit (Gentra Systems, Minneapolis, MN). The supernatant was centrifuged at 12,000 × *g* for 10 minutes at 4°C to pellet the mitochondria. mtDNA was purified by alkaline lysis as in Tamura (38). nDNA concentration was determined by absorbance at 260 nm. mtDNA concentration was determined by the following procedure (because the quantity of DNA was too low for absorbance measurement). The DNA preparation (2-3 μL) was digested with *Bam*HI (New England Biolabs, Beverly, MA) to linearize the circular DNA and electrophoresed on a high sensitivity agarose gel (Reliant HS Gel System, Cambrex, East Rutherford, NJ). The linearized band was scanned and quantified using an imaging system (Alpha Innotech, San Leandro, CA) along with bands of known mass from a DNA ladder (MassRuler, Fermentas, Burlington, Ontario, Canada) on the same gel.

Table 1. Cisplatin sensitivity, Bcl-2 protein expression, glutathione levels, and platinum/DNA adduct formation in cell lines PCI-13 and PCI-51

	PCI-13	PCI-51
Cisplatin IC_{50} (μmol/L)	0.3	3
Bcl-2	–	+
GSH, whole cell (+BSO)	5.3 (0.05) pmol/μg	6.8 (1.7) pmol/μg
GSH, mitochondrial (+BSO)	0.2 (0.05) pmol/μg	1.2 (0.3) pmol/μg

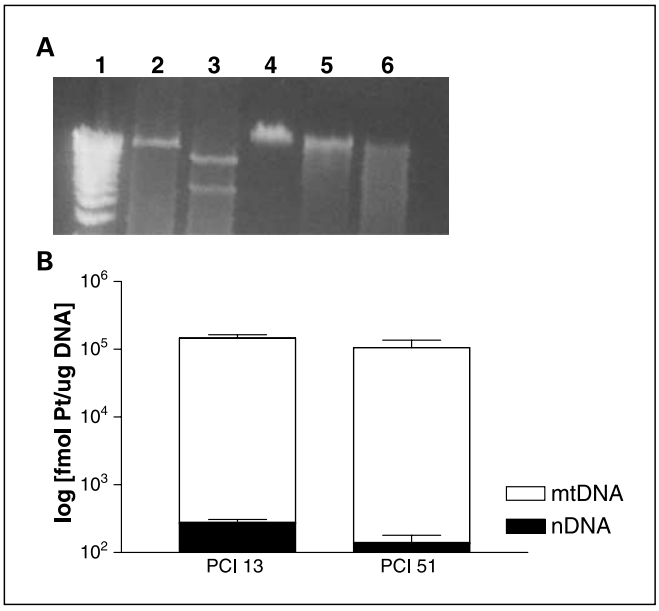

Fig. 1. *A,* agarose gel of mtDNA and nDNA purified from HNSCC cell lines. *Lane 1,* 1 kb DNA ladder; *lane 2,* mtDNA digested with *Bam*HI, producing a linear molecule of 16.6 kb; *lane 3,* mtDNA digested with *Hin*dIII, producing fragments of 5.7 and 10.0 kb (a third fragment of 890 bp is not shown); *lane 4,* undigested nDNA; *lane 5*, nDNA digested with *Bam*HI; *lane 6,* nDNA digested with *Hin*dIII. *B,* levels of platinum detected by atomic absorption spectroscopy in mtDNA and nDNA of PCI-13 and PCI-51 cells. Columns, mean of duplicate measurements from a single assay; bars, SE. Results are representative of three independent experiments. Note logarithmic scale.

The absorbance values of the known bands were used to create a standard curve from which the DNA content of the mitochondrial band was determined. Platinum adduct content was measured by flameless atomic absorption spectroscopy as described (11). Platination measurements were made in duplicate.

Bcl-2 transfection of head and neck squamous cell carcinoma. PCI-13 cells (which are Bcl-2 negative) were transfected with a full-length cDNA for Bcl-2 as described by us previously (13).

PCR analysis of mtDNA. The mtDNA content of PCI-13 wild-type and ρ^0 cells was determined by PCR with primers specific to human mtDNA (upstream, 5′-CCTAGGGATAACAGCGCAAT; downstream, 5′-TAGAAGAGCGATGGTGAGAG). nDNA was detected using primers for the *insulin-like growth factor-II* gene (upstream, 5′-TGGCCTGGACTTGAGTCC; downstream, 5′-CTCTGACTGCTCTGTGAT). Reactions (50 μL) contained 25 μL Herculase Hotstart PCR Master Mix (Stratagene, La Jolla, CA), 100 ng DNA, and 16 pmol of each primer. Reaction cycles were as follows: initial cycle, 5 minutes at 94°C; 30 cycles [30 seconds at 94°C, 30 seconds at 60°C, 40 seconds at 72°C]; final cycle, 5 minutes at 72°C.

Western blotting. For cytochrome *c* immunoblots, samples were prepared as described above. For cox II immunoblots, lysates were prepared from parental and ρ^0 cells harvested by scraping on ice. Cells were washed twice with cold PBS, pelleted at 1,500 × *g* at 4°C, and resuspended in lysis buffer [1% NP40, 1% sodium deoxycholate, 0.1% SDS, 150 mmol/L NaCl, 10 mmol/L Na_2HPO_4 (pH 7.4)]. Proteins were separated by SDS-PAGE and transferred to nitrocellulose. Immunoblotting was done with primary antibodies at the indicated dilutions: cox II, 1:1,000 (anti-Oxphos complex IV subunit II, clone 12C4, Molecular Probes, Eugene, OR); cytochrome *c*, 1:200 (anti–holocytochrome *c*, clone 2CYTC-199, R&D Systems, Minneapolis, MN); and hsp70, 1:20,000 (anti–heat shock protein 70, clone BRM-22, Sigma-Aldrich). Horseradish peroxidase–conjugated anti-mouse IgG (Amersham Biosciences, Piscataway, NJ) was applied 1:10,000 and detected using enhanced chemiluminescence plus (Amersham Biosciences).

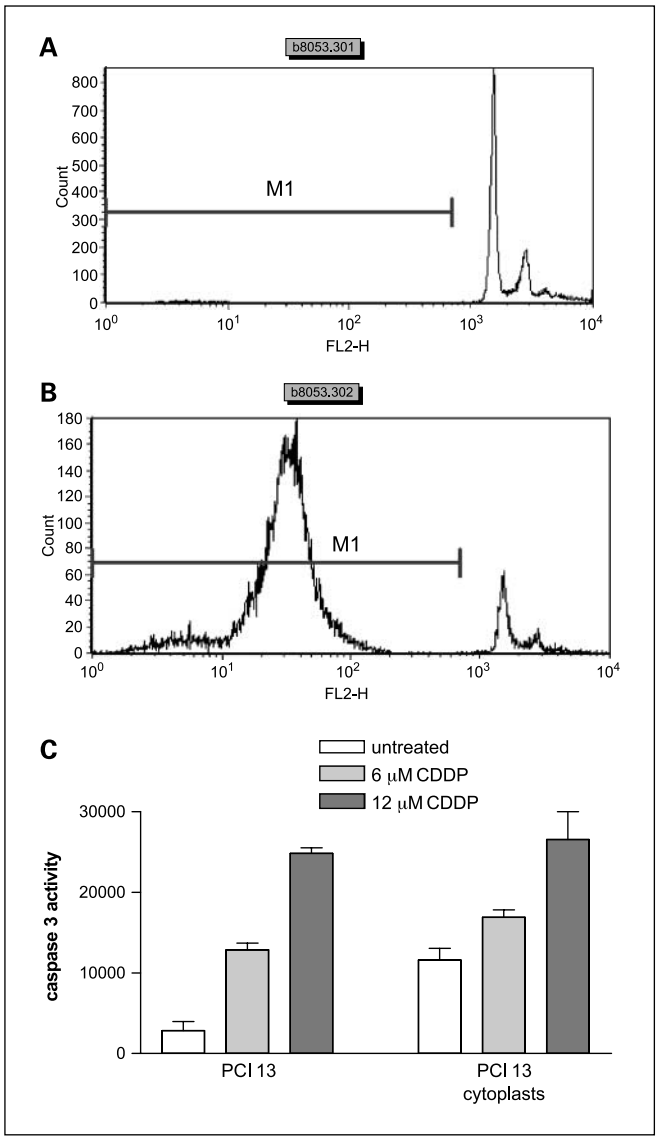

Fig. 2. Detection of active apoptotic pathway in cell cytoplasts. *A* and *B,* flow cytometry of propidium iodide fluorescence in PCI-13 cells (*A*) and cytoplasts (*B*). Cells (91%) in the cytoplast preparation lacked nuclei (region M1). *C,* cisplatin (*CDDP*) treatment induced dose-dependent caspase activity in enucleated cytoplasts as well as in whole cells. Columns, mean of duplicate measurements in a single assay; bars, SE. Results are representative of two independent experiments. Results are in relative fluorescence units. Caspase induction by cisplatin was statistically significant in both intact cells and cytoplasts (one-way ANOVA analysis: whole cells, $P = 0.0001$; cytoplasts, $P = 0.0237$).

Electron microscopy. PCI-13 cells in T75 flasks were treated with 50 μmol/L cisplatin in DMEM supplemented with 10% fetal bovine serum and 2 mmol/L glutamine for the indicated time. Before fixation, the cell monolayer was washed thrice with PBS. Fixative (2.5% glutaraldehyde and 2% paraformaldehyde in 5 mL PBS) was added to the flask for 30 minutes at room temperature and then replaced with PBS for three 5-minute washes. Cells were collected by scraping and pelleted (1,500 × *g*, room temperature) with 2% agarose in PBS. Cell pellets were postfixed in 1% osmium tetroxide for 1 hour and washed with distilled water and en bloc stained with 2% uranyl acetate for 30 minutes in darkness. Samples were dehydrated with graded ethanols and propylene oxide, then embedded in a mixture of Epon 812 substitute and Spurr (Sigma-Aldrich), and polymerized overnight in an oven at 65°C. Ultrathin sections (90 nm) were cut on a Reichert-Jung microtome (Vienna, Austria) and transferred onto copper grids. Grids with sections were stained with lead citrate and examined under a Hitachi H7600 transmission electron microscope (Hitachi, Tokyo, Japan) at 60 kV. Photos were taken with a 6.7-megapixel AMT digital camera (Advanced Microscopy Techniques Corp., Danvers, MA).

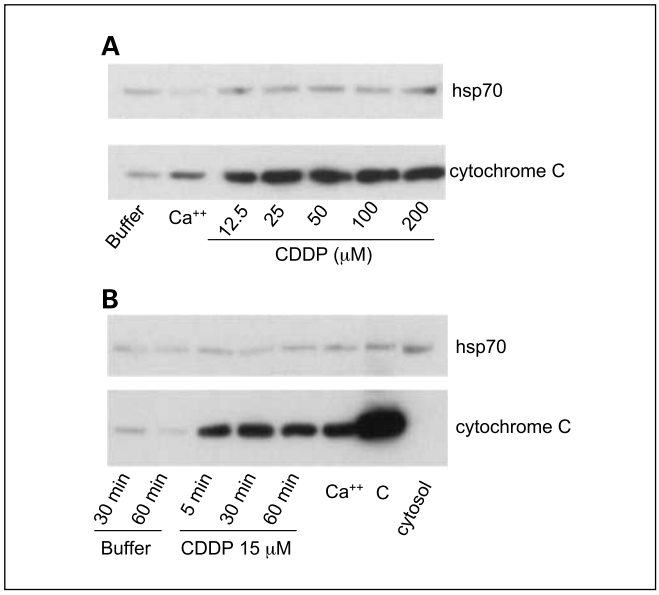

Fig. 3. *A,* Western blot analysis of cisplatin-induced cytochrome *c* release from isolated rat liver mitochondria. Cytochrome *c* was measured in the supernatant of isolated mitochondria treated with cisplatin (CDDP) as indicated. *B,* time course of cytochrome *c* release from isolated rat liver mitochondria treated with 15 μmol/L cisplatin.

Measurement of cisplatin binding to cell and mitochondrial fractions by atomic absorption spectrometry. Head and neck squamous cell carcinoma (HNSCC) cell line PCI-13 was exposed to 50 μmol/L cisplatin for 1 hour at 37°C. After cisplatin exposure, cells were

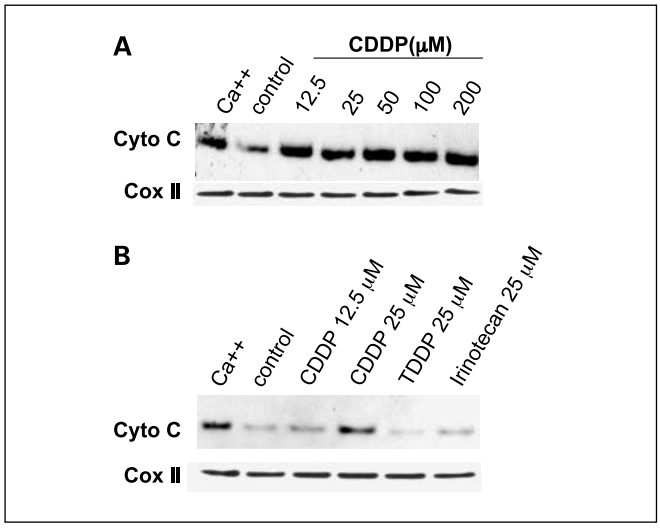

Fig. 4. Cytochrome *c* is rapidly released from HNSCC mitochondria treated with increasing doses of cisplatin; mitochondria from cisplatin-sensitive head and neck cancer cell line PCI-13 were treated with increasing doses of cisplatin for 40 minutes at 30°C. Supernatant from the treated mitochondria was collected and assayed for cytochrome *c* release by Western blot. Cisplatin doses as low as 12.5 μmol/L cause significant cytochrome *c* release. *A,* whereas cisplatin induced rapid cytochrome *c* (*Cyto C*) release, an identical dose of the inactive stereoisomer transplatin (TDDP) did not. *B,* similarly, a cytocidal dose of the topoisomerase I inhibitor irinotecan did not cause significant cytochrome *c* release from mitochondria.

harvested, washed to remove unbound cisplatin, and fractionated as follows. Whole-cell lysate was prepared from one tenth of the cells by standard detergent lysis. Whole-cell protein was prepared by DNase treatment of the whole-cell lysate. The rest of the cells were used to prepare isolated mitochondria by centrifugal fractionation as described for Fig. 3. One tenth of the mitochondrial preparation was used to prepare mitochondrial protein lysate in lysis buffer containing 1% Triton X-100. Voltage-dependent anion channel (VDAC) was isolated to homogeneity from the remaining mitochondrial preparation by affinity chromatography (Fig. 7; ref. 39) This method isolates all VDAC isoforms (1–3). VDAC concentration was estimated by SDS-PAGE from a standard curve of protein mass standards on the same gel. Cisplatin content in all samples was measured by atomic absorption spectrometry as described previously.

Results

Head and neck cell lines for nuclear and mitochondrial analysis. Table 1 presents relevant characteristics of two HNSCC cell lines, PCI-51 and PCI-13, selected for analysis of mtDNA platination based on our previous studies. PCI-51 overexpresses Bcl-2. Its cisplatin IC_{50} is 3 μmol/L. Cell line PCI-13 has a cisplatin IC_{50} of 0.3 μmol/L and is Bcl-2 negative. Whole-cell extracts of PCI-51 contained slightly elevated levels of glutathione compared with PCI-13 (6.8 and 5.3 pmol/μg, respectively). However, mitochondrial glutathione content was 6-fold higher in line PCI-51 compared with PCI-13.

Nuclear versus mitochondrial cisplatin/DNA adducts in head and neck tumor cell lines. Following treatment of PCI-13 and PCI-51 cells for 1 hour with 50 μmol/L cisplatin, cells were harvested and mtDNA and nDNA were purified separately as described. Agarose gel electrophoresis showed that mtDNA was highly purified with minimal nDNA contamination (Fig. 1A). Our results showed that any contaminating nDNA in the mtDNA samples would generate an insignificant contribution to the level of adducts measured in mtDNA (see below).

In the representative experiment shown in Fig. 1B, the cisplatin adduct level in the nDNA of PCI-13 and PCI-51 cells was 116 ± 1 fmol/μg and 121 ± 21 fmol/μg, respectively, whereas the level of cisplatin adducts in mtDNA was 40,700 ± 12,800 fmol/μg and 34,000 ± 3,500 fmol/μg, respectively.

Regardless of time of treatment (1 or 2 hours), pretreatment with BSO to deplete glutathione, or removal of drug for 24 hours to allow DNA repair, the level of adducts in mtDNA in both cell lines was consistently at least 2 orders of magnitude greater than the level in nDNA. mtDNA platinum adducts were a mean of 460 ± 160 times greater in PCI-13 (n = 14) and 350 ± 200 times greater in PCI-51 (n = 12). Consistent with our previous published results (11), pretreatment of both PCI-13 and PCI-51 cells with BSO resulted in a significant enhancement of cisplatin-induced cytotoxicity but no significant difference in cisplatin DNA adducts either in the nucleus or in the mitochondria (data not shown).

PCI-13 nucleus-free cytoplasts retain dose-dependent cisplatin sensitivity. PCI-13 cytoplasts were obtained through the centrifugation technique described in Materials and Methods. Following centrifugation, the nucleus was removed from 91% of the cells as confirmed by flow cytometry (Fig. 2B). Despite the absence of a nucleus, the cell cytoplasts retained dose-dependent cisplatin sensitivity as determined by caspase-3 activation. Although the cytoplasts show a somewhat elevated basal level of caspase-3 activation, they maintained a statistically significant response to escalating doses of cisplatin when compared with the parental cell line (Fig. 2C).

Cisplatin induces rapid dose-dependent release of cytochrome c from mitochondria isolated from rat liver or human HNSCC. Western blot analysis showed dose-dependent release of cytochrome c from isolated rat liver mitochondria into the supernatant (Fig. 3A). Substantial release occurred at the physiologically relevant dose of 12.5 μmol/L cisplatin [peak plasma platinum levels of 10 to 20 μmol/L are achieved clinically (40, 41)] and increased to maximal at doses of ≥25 μmol/L. At a dose of 15 μmol/L cisplatin, cytochrome c release was seen within as little as 5 minutes of cisplatin exposure (Fig. 3B). Similarly, mitochondria isolated from human HNSCC release cytochrome c into the supernatant after brief (40 minutes) exposure to CDDP in a dose-dependent fashion (Fig. 4A and B). Whereas cisplatin induced cytochrome c release, identical doses of the inactive transplatin or the topoisomerase inhibitor irinotecan did not cause release of cytochrome c. This dose of irinotecan is lethal to HNSCC

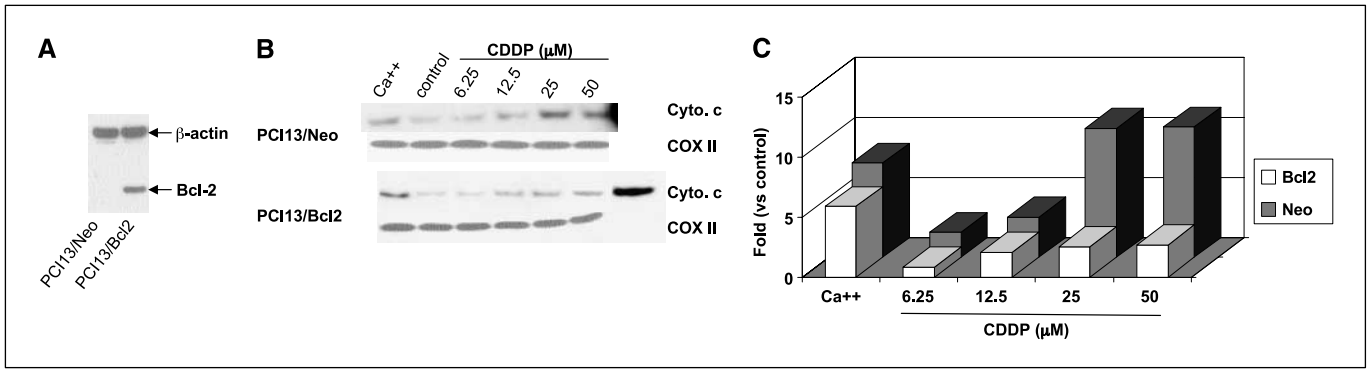

Fig. 5. Mitochondrial Bcl-2 overexpression inhibits cisplatin-induced cytochrome c release. PCI-13 cells were then transfected with the pSFFVNeo vector containing either no insert (PCI-13-neo) or Bcl-2 (PCI-13-Bcl-2) expression construct. *A*, stable expression clones were selected by 400 μg/mL G418 up to 2 weeks and screened by Western blotting using mouse monoclonal antibody against Bcl-2. Sensitivity to cisplatin in PCI-13-neo and PCI-13-Bcl-2 cell clones was tested by semiquantitatively examining the cytochrome c release from isolated mitochondria after cisplatin treatment at 30°C for 40 minutes. Increased release of cytochrome c in PCI-13-neo cells after cisplatin treatment was observed in the cisplatin dose as low as 6.25 μmol/L, whereas in PCI-13-Bcl-2 cells no significantly increased release of cytochrome c was observed after various doses of cisplatin treatment as shown by both Western blotting (*B*) and quantitative densitometry analysis of Western blotting signal intensity (*C*). Release of cytochrome c in PCI-13-neo cells was dosage dependent with dramatically increasing at cisplatin concentration of 25 μmol/L. The mitochondrial gene product cox II was used as a normalization control in Western blotting and densitometry analysis.

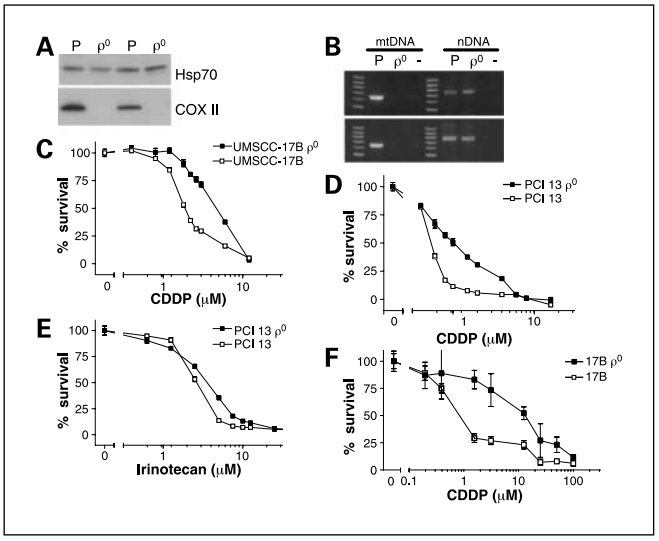

Fig. 6. ρ^0 (mtDNA depleted) cell lines are resistant to cisplatin. *A,* cox II Western blot showing absence of mitochondrially coded protein in ρ^0 cell lines. Lane 1, parental PCI-13 cells; lane 2, PCI-13 ρ^0 cells; lane 3, parental UMSCC-17B cells; lane 4, UMSCC-17B ρ^0 cells. *B,* PCR to detect mtDNA (*lanes 2-4*) and nDNA (*lanes 6-8*) in PCI-13 (*top*) and UMSCC-17B (*bottom*) parental and ρ^0 cell lines. −, PCR, including primers, but no DNA. *C, D,* and *E,* XTT cytotoxicity assays (continuous CDDP exposure). Each is representative of at least three independent experiments. mtDNA absence was confirmed by PCR as in (*B*) before each assay. *C,* cisplatin dose response of UMSCC-17B parental and ρ^0 cells. ρ^0 cells are 3.3-fold resistant at the IC_{50} (5.5 versus 1.8 μmol/L) and 4.5-fold resistant at the IC_{80} (12.7 versus 2.8 μmol/L). *D,* cisplatin dose response of PCI-13 parental and ρ^0 cells. ρ^0 cells are 2.1-fold resistant at the IC_{50} (1.2 versus 0.56 μmol/L) and 4.9-fold resistant at the IC_{80} (3.6 versus 0.74 μmol/L). *E,* irinotecan dose response of PCI-13 parental and ρ^0 cells. ρ^0 IC_{50}, 2.5 ± 0.06 μmol/L; parental IC_{50}, 3.4 ± 0.2 μmol/L. *F,* clonogenic assay of UMSCC-17B and UMSCC-17B ρ^0 cells following 1 hour of cisplatin exposure. In this experiment, mitochondrially depleted UMSCC-17B ρ^0 cells are approximately one log more resistant to cisplatin than the parental cells. This mirrors the results seen in the continuous exposure experiment.

(Fig. 6D), suggesting that the cisplatin effect on mitochondria is specific.

Bcl-2-overexpression blocks cisplatin-mediated cytochrome c release. Mitochondria isolated from human HNSCC cells, which were transfected to overexpress Bcl-2 (Fig. 5A), release significantly less cytochrome *c* after cisplatin treatment compared with wild-type controls (Fig. 5B and C).

mtDNA depletion results in significant cisplatin resistance. To deplete mtDNA from head and neck tumor lines, two cisplatin-sensitive cell lines, PCI-13 and UMSCC-17B cells, were cultured for 20 passages in ethidium bromide. Following ethidium bromide treatment, loss of mtDNA was confirmed by analysis of the expression of the mitochondrially encoded protein cox II as well as by PCR specific to the mtDNA molecule. Ethidium bromide treatment was associated with loss of cox II expression as determined by Western blot (Fig. 6A). PCR analysis showed complete loss of mtDNA product (Fig. 6B). In the nDNA fraction obtained from the same cells, a nuclear control gene (*insulin-like growth factor-II*) was amplified both in the wild-type and ethidium bromide–treated cells (Fig. 6B).

The resulting cells depleted of mtDNA (ρ^0) were evaluated for sensitivity to cisplatin. Both PCI-13 and UMSCC-17B ρ^0 cells showed significant cisplatin resistance compared with parental controls (Fig. 6C). At the IC_{50}, the ρ^0 cell lines were 2- to 3-fold resistant, and at the IC_{80}, both ρ^0 cell lines were 4- to 5-fold resistant. PCI-13 ρ^0 showed an IC_{50} of 1.2 ± 0.2 μmol/L (mean ± SE) and an IC_{80} of 3.6 ± 0.7 μmol/L, whereas the parental values were 0.56 ± 0.03 μmol/L and 0.74 ± 0.04 μmol/L, respectively; UMSCC-17B ρ^0 had IC_{50} and IC_{80} values of 5.5 ± 0.8 μmol/L and 12.7 ± 1.8 μmol/L compared with parental values of 1.8 ± 0.05 μmol/L and 2.8 ± 0.08 μmol/L. As a control, the cytotoxicity of irinotecan, which targets topoisomerase I in the nucleus, was also assayed in PCI-13 parental and ρ^0 cells. As expected, there was little difference in response to this drug in cells depleted of mtDNA (Fig. 6).

Ultrastructural changes in mitochondria are evident by 4 hours after treatment with cisplatin. PCI-13 cells treated with 50 μmol/L cisplatin for 1 and 4 hours were examined by electron microscope (Fig. 7). Cells in each group consistently displayed the features evident in the images presented (at least 10 cells were examined at high resolution in each sample). At 1 hour, no change in mitochondrial or nuclear morphology is seen. Mitochondria in the cells treated for 4 hours (Fig. 7C and F) are pale, rounded, and lack defined cristae structure, all consistent with permeability transition and swelling (42). In contrast, nuclei and nucleoli in the same cells are intact.

Cisplatin binds preferentially to mitochondrial proteins, especially VDAC. Atomic absorption spectroscopic analysis of cellular fractions isolated from cisplatin-treated HNSCC (PCI-13) showed that the cisplatin concentration in the mitochondrial protein fraction was 10-fold higher than in the whole-cell protein fraction. Interestingly, the amount of cisplatin bound to VDAC was 24 times higher than in the mitochondrial protein fraction and >200-fold higher than in the whole-cell protein fraction (Table 2). Figure 8 shows the affinity purification of VDAC for this experiment.

Discussion

Although there has been comparatively little study of direct cisplatin action on mitochondria, some studies have indicated that mtDNA-cisplatin adducts may be significantly more common than cisplatin adducts with nDNA in the same cell line treated with the same concentration of cisplatin (43, 44). This has been attributed to a lack of mtDNA repair following cisplatin exposure (45).

Mitochondria, as the sites of aerobic respiration, are the principal generators of reactive oxygen species in the cell. Mitochondria are dependent on glutathione to detoxify reactive oxygen species, preventing oxidative damage (46, 47). Despite this dependence, mitochondria are unable to synthesize glutathione. Glutathione stores within mitochondria are derived from active transport across the mitochondrial membrane against an electrochemical gradient (48). Mitochondrial glutathione concentrations are regulated and have been implicated in apoptotic regulation (49, 50). At baseline, the concentration of glutathione in mitochondria has been found to be similar to that of the cytoplasm. However, in cells exposed to oxidative stress, the concentration of mitochondrial glutathione is maintained at the expense of a decreasing cytoplasmic pool (51–53). Depletion of the mitochondrial (but not cytoplasmic) glutathione pool is associated with markedly increased sensitivity to antimycin A, which blocks oxidative phosphorylation in complex III of the electron transport chain, leading to generation of reactive oxygen species. These observations suggest that mitochondrial glutathione stores are highly regulated by the cell and may affect the cellular sensitivity to apoptotic stimuli.

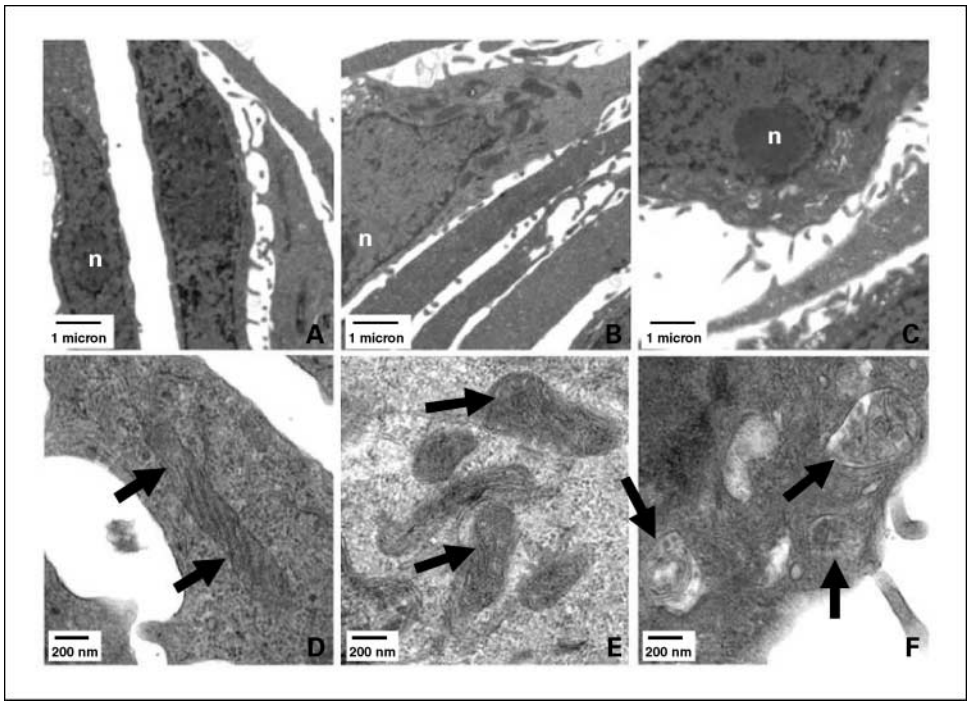

Fig. 7. Electron microscopy of PCI-13 cells treated with cisplatin shows early mitochondrial disruption. *A* and *D,* untreated cells. *B* and *E,* cells treated with 50 μmol/L cisplatin for 1 hour. *C* and *F,* cells treated with 50 μmol/L cisplatin for 4 hours. Arrows, mitochondria. Mitochondrial structure is degraded after 4 hours of cisplatin treatment, whereas nuclear and nucleolar structure at that time point is intact. *D,* mitochondria (*black arrows*) show intact cristae structure with intact inner and outer membrane. *B* and *E,* after 1 hour of treatment, the mitochondria are shortened and there is early distortion of the inner and outer membranes. *C* and *F,* by 4 hours, the cristae are markedly distorted and mitochondrial morphology is completely disrupted, whereas nuclear and nucleolar structure remains unchanged.

Our findings support and expand recent literature reports, which have hinted that cisplatin-induced cytotoxicity may be independent of nDNA binding. In line with our results presented in Fig. 2, Mandic et al. recently showed that enucleated cells retain dose-dependent cisplatin induction of caspase-3 activation in colon and melanoma cell lines. Interestingly, in that study, although the enucleated cells retained sensitivity to cisplatin, they became resistant to the DNA-damaging topoisomerase II inhibitor etoposide (27). Similar results have been reported in colon cancer cell cytoplasts treated with oxaliplatin (54). Other agents may also exert proapoptotic effects through direct interactions with mitochondria (55).

Although we show that head and neck tumor cells lacking mtDNA become cisplatin resistant, they are not completely cisplatin insensitive. A previous study with ρ^0 osteosarcoma cells showed that the loss of mtDNA does not result in a complete absence of cytochrome *c* release from tumor mitochondria when damaged by the toxin staurosporine (56). This result combined with our own suggests that cisplatin-induced mitochondrial toxicity is not entirely DNA dependent. Although we show that mitochondrial platinum adducts are measured at a concentration at least 2 orders of magnitude greater than is measured in the nucleus, the observations that cytochrome *c* release from isolated mitochondria can be seen within 5 minutes of cisplatin exposure and that, in whole cells, ultrastructural damage of mitochondria is clearly visible within a few hours of cisplatin treatment both argue that a direct effect on mitochondrial gene transcription is not necessary for the

Table 2. Cisplatin binding to whole-cell protein, mitochondrial protein, and VDAC protein isolated from cisplatin-treated HNSCC

Fraction	fmol CDDP/μg protein
Whole-cell lysate (included DNA)	256
Whole-cell protein*	7
Mitochondrial protein*	65
VDAC*	1,633

*DNase/RNase treated.

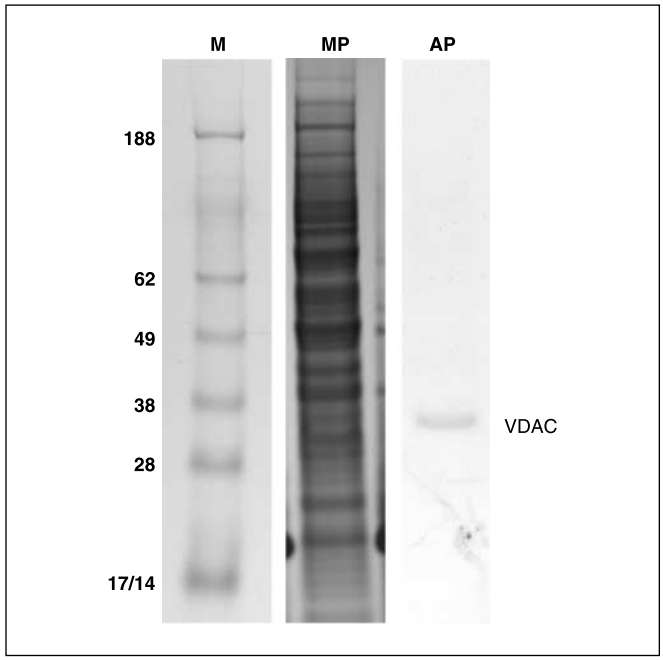

Fig. 8. Cisplatin binds preferentially to mitochondrial proteins, especially VDAC. HNSCC (PCI-13) cells were exposed to 50 μmol/L cisplatin for 1 hour, and various cell fractions were then isolated. Total cisplatin binding to the specific fractions was measured by atomic absorption spectroscopy. VDAC was affinity purified from cisplatin-treated cells as described in the text. M, marker; MP, SDS-PAGE of starting mitochondrial protein fraction; AP, SDS-PAGE of affinity purified VDAC.

mitochondrial toxicity of cisplatin. Importantly, we show that cytochrome *c* release is seen at cisplatin concentrations seen following bolus injection of the drug clinically.

Corresponding to our observation that Bcl-2 transfection is associated with resistance to cisplatin-induced release of cytochrome *c* from the mitochondria, a recent study showed that Bcl-2 overexpression was associated with diminished disruption of mitochondrial ultrastructure following cisplatin treatment as determined by electron microscopy (57). Another recent study of normal middle ear hair cells clearly showed that ototoxicity resulting from cisplatin treatment is associated with severe disruption of mitochondrial structure (58).

Although mitochondria lack the capability for nucleotide excision repair, the marked elevations in mtDNA versus nDNA platinum adducts are not explained by differences in repair alone. Adduct levels in both mtDNA and nDNA decreased at similar rates after cisplatin exposure (data not shown). The electrochemical gradient resulting in a net negative charge within mitochondria may play a role in the significant accumulation of the positively charged cisplatin that we measured. Indeed, alterations in mitochondrial membrane potential have been associated with significant shifts in cisplatin sensitivity (59, 60).

Although we have shown a direct effect of cisplatin on mitochondria, which is not dependent on nuclear or cytoplasmic signaling, our results do not exclude the importance of such effects in generating apoptotic signals following cisplatin exposure. Cisplatin exposure is associated with localization of p53 to the mitochondria, which enhances binding of mitochondrial transcription factor A to cisplatin-damaged mtDNA (61). The p38 mitogen-activated protein kinase pathway may also have a role in cisplatin-induced apoptosis. Activation of p38 has been shown following cisplatin exposure in several studies, and this can be inhibited by RACK1 and AKT2 (62–64).

Cells deficient in nDNA repair are sensitive to cisplatin, but this may be secondary to DNA damage caused by reactive oxygen species generated following release of mitochondrial cytochrome *c*, accelerating apoptosis.

In addition to interacting with nucleophilic sites in DNA, cisplatin binds to nucleophilic amino acid residues in proteins, including cysteine, methionine, and histidine. Cross-linking or modification of critical intracellular proteins by cisplatin is a potentially important, and little studied, cytotoxic mechanism. The effect of cisplatin on mitochondria may be mediated through protein modification or cross-linking. Components of the permeability transition pore, such as the VDAC and the adenine nucleotide translocator, are interesting candidates. Both contain vulnerable residues, and modification of a cysteine residue of adenine nucleotide translocator by thiol cross-linking agents has been shown to cause mitochondrial membrane permeabilization and apoptosis (65). Our finding that the concentration of cisplatin bound to VDAC is more 200-fold higher than the amount bound by total cellular proteins raises the interesting possibility that cisplatin binding to this key mitochondrial membrane protein could significantly alter its structure or function, facilitating the release of cytochrome *c*.

In conclusion, our data indicate that, in HNSCC cell lines, the cytotoxic effect of cisplatin is, in significant part, mediated through direct action on mitochondria. Although cisplatin interactions with nDNA may have important cellular effects contributing to apoptosis, cisplatin binding to nDNA is not necessary for induction of apoptosis. Indeed, the data presented here, in combination with recent findings discussed above, suggest that mitochondria may be the principal and sufficient target of cisplatin in this group of diseases. Further studies will be necessary to determine the precise mitochondrial target(s) of cisplatin and whether these observations are applicable to other tumor types. In the future, mitochondria-based drug screening assays may be important in the evaluation of new chemotherapeutic agents.

Acknowledgments

We thank Drs. Willhelm Bohr, Gary Fiskum, Edward Sausville, and Christos Chinopoulos for their critical comments and Lombardi Comprehensive Cancer Center microscopy core facility for the technical assistance.

References

1. Andrews PA, Howell SB. Cellular pharmacology of cisplatin: perspectives on mechanisms of acquired resistance. Cancer Cell 1990;2:35–43.
2. Sorenson CM, Eastman A. Influence of *cis*-diamminedichloroplatinum(II) on DNA synthesis and cell cycle progression in excision repair proficient and deficient Chinese hamster ovary cells. Cancer Res 1988; 48:6703–7.
3. Eastman A. Activation of programmed cell death by anticancer agents: cisplatin as a model system. Cancer Cell 1990;2:275–80.
4. Eastman A, Barry MA. The origins of DNA breaks: a consequence of DNA damage, DNA repair, or apoptosis? Cancer Invest 1992;10:229–40.
5. Fuertes MA, Castilla J, Alonso C, Perez JM. Cisplatin biochemical mechanism of action: from cytotoxicity to induction of cell death through interconnections between apoptotic and necrotic pathways. Curr Med Chem 2003;10:257–66.
6. Gonzalez VM, Fuertes MA, Alonso C, Perez JM. Is cisplatin-induced cell death always produced by apoptosis? Mol Pharmacol 2001;59:657–63.
7. Crul M, van Waardenburg RC, Beijnen JH, Schellens JH. DNA-based drug interactions of cisplatin. Cancer Treat Rev 2002;28:291–303.
8. Kartalou M, Essigmann JM. Mechanisms of resistance to cisplatin. Mutat Res 2001;478:23–43.
9. Bier H. Circumvention of drug resistance in cisplatin-resistant sublines of the human squamous carcinoma cell line HLac 79 *in vitro* and *in vivo*. Acta Otolaryngol 1991;111:797–806.
10. Andrews PA, Schiefer MA, Murphy MP, Howell SB. Enhanced potentiation of cisplatin cytotoxicity in human ovarian carcinoma cells by prolonged glutathione depletion. Chem Biol Interact 1988;65:51–8.
11. Yang Z, Faustino PJ, Andrews PA, et al. Decreased cisplatin/DNA adduct formation is associated with cisplatin resistance in human head and neck cancer cell lines. Cancer Chemother Pharmacol 2000;46: 255–62.
12. Isonishi S, Saitou M, Yasuda M, Tanaka T. Mitochondria in platinum resistant cells. Hum Cell 2001;14: 203–10.
13. Rudin CM, Yang Z, Schumaker LM, et al. Inhibition of glutathione synthesis reverses Bcl-2-mediated cisplatin resistance. Cancer Res 2003;63:312–8.
14. Liang BC, Ullyatt E. Increased sensitivity to *cis*-diamminedichloroplatinum induced apoptosis with mitochondrial DNA depletion. Cell Death Differ 1998; 5:694–701.
15. Park SY, Chang I, Kim JY, et al. Resistance of mitochondrial DNA-depleted cells against cell death: role of mitochondrial superoxide dismutase. J Biol Chem 2004;279:7512–20.
16. Preston TJ, Abadi A, Wilson L, Singh G. Mitochondrial contributions to cancer cell physiology: potential for drug development. Adv Drug Deliv Rev 2001;49: 45–61.
17. Kim T-S, Yun BY, Kim IY. Induction of the mitochondrial permeability transition by selenium compounds mediated by oxidation of the protein thiol groups and generation of the superoxide. Biochem Pharmacol 2003;66:2301–11.
18. Chilin A, Dodoni G, Frezza C, et al. 4-hydroxymethyl-1,6,8-trimethylfuro[2,3-h]quinolin-2(1H)-one induces mitochondrial dysfunction and apoptosis upon its intracellular oxidation. J Med Chem 2005; 48:192–9.
19. Keshavan P, Schwemberger SJ, Smith DL, Babcock GF, Zucker SD. Unconjugated bilirubin induces apoptosis in colon cancer cells by triggering mitochondrial depolarization. Int J Cancer 2004;112:433–45.
20. Zheng Y, Yamaguchi H, Tian C, et al. Arsenic trioxide (As(2)O(3)) induces apoptosis through activation of Bax in hematopoietic cells. Oncogene 2005;24: 3339–47.
21. Oliver CL, Miranda MB, Shangary S, Land S, Wang S, Johnson DE. (−)-Gossypol acts directly on the mitochondria to overcome Bcl-2- and Bcl-X(L)-mediated apoptosis resistance. Mol Cancer Ther 2005;4:23–31.

22. Rotem R, Heyfets A, Fingrut O, Blickstein D, Shaklai M, Flescher E. Jasmonates: novel anticancer agents acting directly and selectively on human cancer cell mitochondria. Cancer Res 2005;65:1984–93.

23. Yanez JA, Teng XW, Roupe KA, Fariss MW, Davies NM. Chemotherapy induced gastrointestinal toxicity in rats: involvement of mitochondrial DNA, gastrointestinal permeability, and cyclooxygenase-2. J Pharm Pharm Sci 2003;6:308–14.

24. Devarajan P, Savoca M, Castaneda MP, et al. Cisplatin-induced apoptosis in auditory cells: role of death receptor and mitochondrial pathways. Hear Res 2002;174:45–54.

25. Park MS, De Leon M, Devarajan P. Cisplatin induces apoptosis in LLC-PK1 cells via activation of mitochondrial pathways. J Am Soc Nephrol 2002;13:858–65.

26. Schwerdt G, Freudinger R, Schuster C, Silbernagl S, Gekle M. Inhibition of mitochondria prevents cell death in kidney epithelial cells by intra- and extracellular acidification. Kidney Int 2003;63:1725–35.

27. Jacobson MD, Burne JF, Raff MC. Programmed cell death and Bcl-2 protection in the absence of a nucleus. EMBO J 1994;13:1899–910.

28. Mandic A, Hansson J, Linder S, Shoshan MC. Cisplatin induces endoplasmic reticulum stress and nucleus-independent apoptotic signaling. J Biol Chem 2003;278:9100–6.

29. Marchetti P, Zamzami N, Joseph B, et al. The novel retinoid 6-[3-(1-adamantyl)-4-hydroxyphenyl]-2-naphtalene carboxylic acid can trigger apoptosis through a mitochondrial pathway independent of the nucleus. Cancer Res 1999;59:6257–66.

30. Bossy-Wetzel E, Green DR. Caspases induce cytochrome *c* release from mitochondria by activating cytosolic factors. J Biol Chem 1999;274:17484–90.

31. Deveraux QL, Takahashi R, Salvesen GS, Reed JC. X-linked IAP is a direct inhibitor of cell-death proteases. Nature 1997;388:300–4.

32. Tietze F. Enzymic method for quantitative determination of nanogram amounts of total and oxidized glutathione: applications to mammalian blood and other tissues. Anal Biochem 1969;27:502–22.

33. Amuthan G, Biswas G, Ananadatheerthavarada HK, Vijayasarathy C, Shephard HM, Avadhani NG. Mitochondrial stress-induced calcium signaling, phenotypic changes, and invasive behavior in human lung carcinoma A549 cells. Oncogene 2002;21:7839–49.

34. Armand R, Channon JY, Kintner J, et al. The effects of ethidium bromide induced loss of mitochondrial DNA on mitochondrial phenotype and ultrastructure in a human leukemia T-cell line (MOLT-4 cells). Toxicol Appl Pharmacol 2004;196:68–79.

35. King MP, Attardi G. Isolation of human cell lines lacking mitochondrial DNA. Methods Enzymol 1996;264:304–13.

36. King MP, Attardi G. Human cells lacking mtDNA: repopulation with exogenous mitochondria by complementation. Science 1989;246:500–3.

37. Jacobson MD, Burne JF, King MP, Miyashita T, Reed JC, Raff MC. Bcl-2 blocks apoptosis in cells lacking mitochondrial DNA. Nature 1993;361:365–9.

38. Tamura K, Aotsuka T. Rapid isolation method of animal mitochondrial DNA by the alkaline lysis procedure. Biochem Genet 1988;26:815–9.

39. Baker MA, Lane DJ, Ly JD, DePinto V, Lawen A. VDAC1 is a transplasma membrane NADH-ferricyanide reductase. J Biol Chem 2004;279:4811–9.

40. Patton TF, Repta AJ, Sternson LA. Clinical pharmacology of cisplatin. In: Ames MM, Powis G, Kovach JS, editors. Pharmacokinetics of anticancer agents in humans. New York: Elsevier; 1983.

41. Andersson A, Fagerberg J, Lewensohn R, Ehrsson H. Pharmacokinetics of cisplatin and its monohydrated complex in humans. J Pharm Sci 1996;85:824–7.

42. von Ahsen O, Renken C, Perkins G, Kluck RM, Bossy-Wetzel E, Newmeyer DD. Preservation of mitochondrial structure and function after Bid- or Bax-mediated cytochrome *c* release. J Cell Biol 2000;150:1027–36.

43. Murata T, Hibasami H, Maekawa S, Tagawa T, Nakashima K. Preferential binding of cisplatin to mitochondrial DNA and suppression of ATP generation in human malignant melanoma cells. Biochem Int 1990;20:949–55.

44. Olivero OA, Semino C, Kassim A, Lopez-Larraza DM, Poirier MC. Preferential binding of cisplatin to mitochondrial DNA of Chinese hamster ovary cells. Mutat Res 1995;346:221–30.

45. Singh G, Maniccia-Bozzo E. Evidence for lack of mitochondrial DNA repair following *cis*-dichlorodiammineplatinum treatment. Cancer Chemother Pharmacol 1990;26:97–100.

46. Davis W, Jr., Ronai Z, Tew KD. Cellular thiols and reactive oxygen species in drug-induced apoptosis. J Pharmacol Exp Ther 2001;296:1–6.

47. Anderson ME. Glutathione: an overview of biosynthesis and modulation. Chem Biol Interact 1998;111–112:1–14.

48. Griffith OW, Meister A. Origin and turnover of mitochondrial glutathione. Proc Natl Acad Sci U S A 1985;82:4668–72.

49. Martensson J, Meister A. Mitochondrial damage in muscle occurs after marked depletion of glutathione and is prevented by giving glutathione monoester. Proc Natl Acad Sci U S A 1989;86:471–5.

50. Martensson J, Jain A, Stole E, Frayer W, Auld PA, Meister A. Inhibition of glutathione synthesis in the newborn rat: a model for endogenously produced oxidative stress. Proc Natl Acad Sci U S A 1991;88:9360–4.

51. Fernandez-Checa JC, Kaplowitz N, Garcia-Ruiz C, et al. GSH transport in mitochondria: defense against TNF-induced oxidative stress and alcohol-induced defect. Am J Physiol 1997;273:G7–17.

52. Colell A, Garcia-Ruiz C, Morales A, et al. Transport of reduced glutathione in hepatic mitochondria and mitoplasts from ethanol-treated rats: effect of membrane physical properties and S-adenosyl-L-methionine. Hepatology 1997;26:699–708.

53. Garcia-Ruiz C, Colell A, Morales A, Kaplowitz N, Fernandez-Checa JC. Role of oxidative stress generated from the mitochondrial electron transport chain and mitochondrial glutathione status in loss of mitochondrial function and activation of transcription factor nuclear factor-κB: studies with isolated mitochondria and rat hepatocytes. Mol Pharmacol 1995;48:825–34.

54. Gourdier I, Crabbe L, Andreau K, Pau B, Kroemer G. Oxaliplatin-induced mitochondrial apoptotic response of colon carcinoma cells does not require nuclear DNA. Oncogene 2004;23:7449–57.

55. Kluza J, Gallego M, Loyens A, et al. Cancer cell mitochondria are direct proapoptotic targets for the marine antitumor drug lamellarin D. Cancer Res 2006;66:3177–87.

56. Jiang S, Cai J, Wallace DC, Jones DP. Cytochrome *c*-mediated apoptosis in cells lacking mitochondrial DNA. Signaling pathway involving release and caspase 3 activation is conserved. J Biol Chem 1999;274:29905–11.

57. de Graaf AO, van den Heuvel LP, Dijkman HB, et al. Bcl-2 prevents loss of mitochondria in CCCP-induced apoptosis. Exp Cell Res 2004;299:533–40.

58. Cardinaal RM, De Groot JC, Huizing EH, Smoorenburg GF, Veldman JE. Ultrastructural changes in the albino guinea pig cochlea at different survival times following cessation of 8-day cisplatin administration. Acta Otolaryngol 2004;124:144–54.

59. Andrews PA, Albright KD. Mitochondrial defects in *cis*-diamminedichloroplatinum(II)-resistant human ovarian carcinoma cells. Cancer Res 1992;52:1895–901.

60. Zinkewich-Peotti K, Andrews PA. Loss of *cis*-diamminedichloroplatinum(II) resistance in human ovarian carcinoma cells selected for rhodamine 123 resistance. Cancer Res 1992;52:1902–6.

61. Yoshida Y, Izumi H, Torigoe T, et al. P53 physically interacts with mitochondrial transcription factor A and differentially regulates binding to damaged DNA. Cancer Res 2003;63:3729–34.

62. Losa JH, Cobo CP, Viniegra JG, Sanchez-Arevalo Lobo V, Cajal S, Sanchez-Prieto R. Role of the p38 MAPK pathway in cisplatin-based therapy. Oncogene 2003;22:3998–4006.

63. Jeong HG, Cho HJ, Chang IY, et al. Rac1 prevents cisplatin-induced apoptosis through down-regulation of p38 activation in NIH3T3 cells. FEBS Lett 2002;518:129–34.

64. Yuan ZQ, Feldman RI, Sussman GE, Coppola D, Nicosia SV, Cheng JQ. AKT2 inhibition of cisplatin-induced JNK/p38 and Bax activation by phosphorylation of ASK1: implication of AKT2 in chemoresistance. J Biol Chem 2003;278:23432–40.

65. Costantini P, Belzacq AS, Vieira HL, et al. Oxidation of a critical thiol residue of the adenine nucleotide translocator enforces Bcl-2-independent permeability transition pore opening and apoptosis. Oncogene 2000;19:307–14.